AIR MINISTRY
For Official Use

R. & M. No. 1369

AERONAUTICAL RESEARCH COMMITTEE
REPORTS AND MEMORANDA No. 1369
(Ae. 496—T.3062)

FURTHER EXPERIMENTS ON

THE FLOW AROUND A CIRCULAR CYLINDER

By A. FAGE
A.R.C.Sc. AND
V. M. FALKNER
B.Sc.

FEBRUARY, 1931

LONDON:
PRINTED AND PUBLISHED BY HIS MAJESTY'S STATIONERY OFFICE
To be purchased directly from H.M. STATIONERY OFFICE at the following addresses:
Adastral House, Kingsway, London, W.C.2; 120, George Street, Edinburgh;
York Street, Manchester; 1, St. Andrew's Crescent, Cardiff;
15, Donegall Square West, Belfast;
or through any Bookseller.

1931.

Price 1*s.* 0*d.* Net.

23-9999

R5517

AERODYNAMIC SYMBOLS.

1. General

m mass

t time

V resultant linear velocity

Ω resultant angular velocity

ρ density, σ relative density

ν kinematic coefficient of viscosity

R Reynolds number, $R = lV/\nu$ (where l is a suitable linear dimension), to be expressed as a numerical coefficient x 10^6

Normal temperature and pressure for aeronautical work are 15° C. and 760 mm.

For air under these conditions $\begin{cases} \rho = 0{\cdot}002378 \text{ slug/cu. ft.} \\ \nu = 1{\cdot}59 \times 10^{-4} \text{ sq. ft./sec.} \end{cases}$

The slug is taken to be 32·2 lb.-mass.

α angle of incidence

ϵ angle of downwash

S area

c chord

s semi-span

A aspect ratio, $A = 4s^2/S$

L lift, with coefficient $k_L = L/S\rho V^2$

D drag, with coefficient $k_D = D/S\rho V^2$

γ gliding angle, $\tan\gamma = D/L$

L rolling moment, with coefficient $k_l = L/sS\rho V^2$

M pitching moment, with coefficient $k_m = M/cS\rho V^2$

N yawing moment, with coefficient $k_n = N/sS\rho V^2$

...tions per second

...eter

..., with coefficient $k_T = T/\rho n^2 D^4$

..., with coefficient $k_Q = Q/\rho n^2 D^5$

...ncy, $\eta = TV/P = Jk_T/2\pi k_Q$

 1

FOR OFFICIAL USE.

FURTHER EXPERIMENTS ON THE FLOW AROUND A CIRCULAR CYLINDER.

By A. Fage, A.R.C.Sc. and V. M. Falkner, B.Sc.

Reports and Memoranda No. 1369.

(Ae. 496.)

February, 1931.

Summary.—The intensity of friction on the surfaces of two cylinders of diameter 2·93 in. and 5·89 in. respectively have been determined from measurements of velocity taken at distances of about 0·0025 in. from the surface with small surface tubes. The sensitive range of Reynolds number (V_0D/ν) over which large changes in the flow characteristics are experienced was covered in the experiments on the larger cylinder.

The character of the frictional distribution depends on the value of (V_0D/ν). At a relatively low value of ($V_0D\nu$), the frictional intensity rises gradually to a maximum value and then rapidly falls to a zero value; whereas at a larger value of (V_0D/ν) within the sensitive range the frictional intensity after reaching its maximum value falls less abruptly to a minimum value, and then rises to a second maximum before the zero value is reached. A transition from laminar to turbulent flow occurs in the boundary layer where the frictional intensity is a minimum. The transition region is also clearly indicated by a marked inflexion in the curve of pressure distribution.

The frictional distribution measured on the 5·89 in. cylinder is in reasonably close agreement with that predicted by modern boundary layer theory.

Experiments have also been made to determine the effect of disturbances in the general stream on the characteristics of the flow.

Introduction.—In an earlier paper, R. & M. 1179*, an examination of the airflow in the boundary layer around a circular cylinder near the region where the separation from the surface took place was made from observations of total head taken with a small exploring tube. The types of flow considered were those associated with the large change of K_D which occurs at high values of Reynolds number (V_0D/ν). An analysis of these experimental results showed that there was a critical point on the cylinder, just beyond the region of maximum negative pressure, where a transition from laminar to turbulent flow in the boundary layer began, and that

---

* "The airflow around a circular cylinder in the region where the boundary layer separates from the surface."—A. Fage.

the position of this point on the cylinder was indicated by a pronounced inflexion in the curve of normal pressure. In a later paper, R. & M. 1231*, an attempt was made to determine from the experimental data given in the earlier paper, the intensity of friction on a limited part of the surface of the cylinder ($\theta = 40°$ to $90°$) anterior to the region of maximum negative pressure. Since the publication of these two papers an experimental method of measuring the friction on the surface of a body immersed in an air stream from observations of velocity taken with exceedingly small surface tubes has been developed and tested on a large metal aerofoil†. This method was found to be reliable and in view of the success obtained in these experiments on the aerofoil, the Aerodynamics Sub-Committee agreed to a suggestion that further experiments should be made to determine the intensity of friction on the surface of a circular cylinder, and that these experimental results should be compared with results predicted by modern boundary layer theory. The present investigation gives the information desired by the Aerodynamics Sub-Committee. In addition, the results obtained throw more light on the phenomenon of the separation of the boundary layer from the surface of a cylinder and also on the effect of disturbances in the general airstream on the characteristics of the flow around a cylinder.

List of Symbols.

V_0 ≡ velocity in the general airstream.
V ≡ tangential velocity near the surface of the cylinder.
p_0 ≡ pressure in the general airstream.
p ≡ normal pressure at any point on surface.
ρ ≡ density of air.
μ ≡ coefficient of viscosity.
ν ≡ coefficient of kinematic viscosity.
H_0 ≡ total head in the general airstream.
H ≡ total head at any point in the field.
D ≡ diameter of cylinder.
θ ≡ angular position of a point on the surface of cylinder measured from the general wind direction.
y ≡ normal distance from surface of cylinder.
δ ≡ thickness of boundary layer, measured normal to the surface.
$\bar{y}$ ≡ distance of the effective centre of a surface tube from the surface.
K_D ≡ drag coefficient (drag per unit length/$\rho D V_0^2$).
f ≡ intensity of surface friction.

---

* "The skin friction on a circular cylinder."—A. Fage.

† R. & M. 1315. "An experimental determination of the intensity of friction on the surface of an aerofoil."—Fage and Falkner.

Description of Experiments.—The experiments were made on two circular cylinders of diameter 2·93 and 5·89 inches respectively. Each cylinder was mounted with very small clearances between the floor and roof of a 4 ft. Tunnel, and all the velocity and pressure measurements were made at the median section, where the flow was closely two-dimensional. Each cylinder was turned from a steel tube, and finished with a highly polished smooth surface.

The experiments were made with each cylinder mounted in normal wind streams of the tunnel and also in disturbed streams at a distance of about 36 in. behind a rope netting stretched across a section of the tunnel. The diameter of the rope was 0·25 in. and the mesh of the netting 1·5 in.

The experiments on the larger cylinder (5·89 in.) are of special interest for they cover a large part of the sensitive range of Reynolds number (V_0D/ν) over which the flow around the cylinder experiences marked changes in character.

The intensity of surface friction, f, was determined from the relation.

$$f = \mu\left(\frac{\partial V}{\partial y}\right)_{y=0},$$

where μ is the coefficient of viscosity and V the velocity parallel to the surface at a normal distance y from the surface. The value of

$$\left(\frac{\partial V}{\partial y}\right)_{y=0}$$

was obtained from measurements of velocity made very near the surface with small surface tubes of the Stanton type. The characteristic feature of this type of tube is that the inner wall of the tube is formed by the surface itself.

The procedure in the present experiments was the same as that followed in the earlier experiments on the aerofoil. It is not necessary, therefore, since reference can be made to R. & M. 1315, to describe the experiments in detail.

Two tubes were used*. The widths of the mouth openings of these tubes were 0·0044 and 0·0026 inch respectively. Each of these tubes was constructed on the top of a circular rod of diameter 0·2 in., designed to pass with a small clearance through a hole in a cylinder. In practice, a tube was carefully mounted on a cylinder so that the top surface of the rod was flush with the surface of the cylinder. The tubes were calibrated in the laminar flow in a pipe having a rectangular cross-section, and with them it was possible to measure the velocity (V) at points situated at distances ($\bar{y}$) of about 2 to 3 thousandths of an inch from the surface of a cylinder.

---

* One of these tubes was No. 3 of R. & M. 1315.

(5936) Wt. 95/6003/2114 375 7/31 Hw. G. 7/1

In the earlier work on the aerofoil the intensity of surface friction was estimated on the assumption that the velocity in the boundary layer increased linearly from the zero value at the surface to the value (V) measured with a surface tube at the very small distance ($\bar{y}$). The intensity of friction was then given by

$$f = \mu \frac{V}{\bar{y}}$$

This assumption of linearity, which was shown to be reasonably sound in the case of the aerofoil, can obviously only hold provided the boundary layer is not too thin. This condition was not fulfilled on the two cylinders, and an attempt had therefore to be made to predict a relation between the velocity gradient at the surface

$$\left(\frac{\partial V}{\partial y}\right)_{y=0}$$

and the value of ($V/\bar{y}$) obtained from the observations taken with the surface tubes. It will be seen later that there are theoretical grounds for the belief that this relation is given by

$$\left(\frac{\partial V}{\partial y}\right)_{y=0} = 1 \cdot 16 \left(\frac{V}{\bar{y}}\right)$$

The intensity of surface friction was therefore given by the relation

$$f = 1 \cdot 16 \, \mu \left(\frac{V}{\bar{y}}\right)$$

The two series of values of the intensity of surface friction predicted in the manner described above from the observations taken with the two tubes were found to be in close agreement, and accordingly only the mean values are given in the paper. The differences between the individual values and the accepted mean values were within $\pm$ 3·5 per cent. of the mean value.

The mean values of the coefficients of frictional intensity ($f/\rho V_0^2$) are plotted against θ, where θ is the angular position of a point on the surface of a cylinder measured from the general wind direction, in Figs. 1 and 2. The curves of these figures show that the frictional intensity rises to a maximum value near $\theta = 55°$ on the front part of the surface of each cylinder. Beyond this region however the frictional distribution is clearly dependent on the value of the Reynolds number at which the measurements were made and on the nature of the disturbances in the general stream. There appear to be two distinct kinds of distribution. In the first kind, the frictional intensity after attaining its maximum value falls rapidly to a zero value; and in the second, the frictional intensity falls less rapidly to a minimum value and then rises to a second maximum value before the zero value is finally reached. The distributions measured in the normal streams at the lower Reynolds numbers (a, b and c of Fig. 2 and g of Fig. 1) are of the first kind, and those measured in the normal stream at the higher Reynolds numbers (f, and e of Fig. 1) and in the disturbed streams behind the rope netting (h, i of Fig. 1, and d of Fig. 2) are of the second kind.

It is obvious that the point where the frictional intensity falls to its zero value indicates the position on the cylinder where the separation of the boundary layer from the surface is just completed. The fall of the frictional intensity to a minimum value has a special significance, for earlier work on boundary layer problems suggests it is on this region of the surface that a transition from laminar to turbulent flow in the boundary layer takes place. This feature of the flow will be considered again later, when the curves of Fig. 1 are viewed in conjunction with the pressure curves of Fig. 3. Further information gathered from the curves of Fig. 1 which refer to those flows which are sensitive to a change of Reynolds number, is that for this type of flow the addition of artificial disturbances into the normal tunnel stream causes the points of minimum and zero frictional intensity to occur further around the cylinder, and so both the transition from laminar to turbulent flow and the separation of the boundary layer from the surface are delayed. These effects are connected with a change of pressure distribution around the cylinder, but the phenomenon is of interest because it is well known that for flows along pipes and plates, disturbances in the general stream hasten the transition from laminar to turbulent flow.

Normal Pressure.—The distributions of normal pressure on each cylinder are given in Fig. 3. The curves of this figure were obtained by plotting the measured values of $(p-p_0)/\varrho V_0^2$ against $\theta°$, where p is the normal pressure at a point whose angular position is given by $\theta°$, and p_0 is the pressure in the undisturbed stream. The measured values of $(p-p_0)/\varrho V_0^2$ are also given in Table 3 (appended).

The most noticeable feature of the curves of Fig. 3 is the change in the general character of the pressure distribution with an increase of Reynolds number over the sensitive range. Another important trait exhibited is the inflexion in each curve at a point (marked B) just beyond the region of maximum negative pressure. Attention has been previously directed in R. & M. 1179 to this feature, and the conclusion was there drawn that a transition from laminar to turbulent flow took place in the boundary layer near this inflexion. The experimental evidence adduced for this conclusion was the rapid opening-out of the boundary layer and the noticeable change in the radial distributions of total head (and so of velocity) in this region.

The evidence obtained from experiments on flat plates and aerofoils shows that the frictional intensity falls to a minimum on that part of the surface where a transition from laminar to turbulent flow takes place in the boundary layer. If therefore the conclusion drawn in R. & M. 1179 is sound the inflexion in the pressure curve should indicate the position where the frictional intensity falls to a minimum. To allow the relevant parts of the frictional curves of Fig. 1 and those of the pressure curves of Fig. 3 to be viewed in conjunction, they have been replotted on an open scale in Fig. 4. In all cases, the inflexion in a pressure curve is seen to occur where the frictional intensity is a minimum. The additional evidence obtained from the present experiments supports therefore the earlier conclusion that the inflexion in the pressure curve marks the position where the transition from laminar to turbulent flow in the boundary layer takes place.

Separation Region.—Another conclusion drawn in R. & M. 1179 was that at high values of Reynolds number, the separation of the boundary layer from the surface was completed just beyond (about 10°) the position of the point of inflexion (B) in the pressure curve. This conclusion was based on the experimental evidence that the radial gradient of total head at the surface ($\partial (H - H_0)/\partial y$) was very small at the point B, and that beyond this point the total head tended to become constant over an appreciable radial distance from the surface. In order that the point of view taken in R. & M. 1179 may be understood some experimental observations given in that paper are reproduced in Fig. 5. The curves in this figure represent the distributions of total head in the boundary layer of an 8·9 in. cylinder in a wind stream of 71·4 ft./sec. The curves show that the point of inflexion in the pressure curve occurs at $\theta = 96 \cdot 4°$, and that near this position the value of

$$\left[\frac{\partial (H - H_0)}{\partial y}\right]_{y=0}$$

appears to become zero (see curve for $\theta = 94 \cdot 8°$). Further, it was suggested that the separation of the boundary layer from the surface was completed at $\theta = 104°$.

The view that the separation was completed close behind (about 10°) the inflexion point B must now be abandoned, in the light of the additional information obtained from the measurements of frictional intensity. For, the curves of Fig. 4 show that at high values of Reynolds number measurements of surface friction can be made over an appreciable region (about 40°) beyond the point B, and these measurements could not have been made unless the boundary layer were in contact with the surface. As would be expected, the evidence given in Fig. 4 clearly indicates that the region of constant pressure at the back of the cylinder begins immediately after the boundary layer has left the surface of the cylinder (see lines C). The interpretation now placed on the curves of Fig. 5 is that the separation of the boundary layer from the surface is just completed at about $\theta = 130°$, where the total head is constant over a relatively large radial distance from the surface. The progressive change in the shape of the total-head curves between B ($\theta = 96 \cdot 4°$) and C ($\theta = 130°$) is associated with a continuous drop in the frictional intensity, and it is probable that the separation is taking place over the whole of this region.

Theory.—The intensity of friction on the surface of a cylinder can be predicted from a solution of the Prandtl simplified equations for laminar flow in the boundary layer, when the distribution of normal pressure on the surface is known. Several methods for the solution of these equations have been suggested, and of these only those developed in this country will be considered. In R. & M. 1176 Dr. Thom* has given a simple expression for the intensity of friction on that part of the front surface of a cylinder, over which the pressure gradient ($dp/d\theta$) is decreasing. This expression ceases to be valid when the pressure gradient becomes zero or positive. Later, Mr. J. J. Green† of the Royal College of Science has obtained, by the use of step-by-step methods, a solution of the equations for the entire range of laminar flow around a cylinder ; and one of the present authors‡, in collaboration with Miss S. Skan, has obtained some approximate solutions of the equations which are presented in such a form that a direct application to problems, such as the one now under consideration, is reduced to a fairly simple analytical rule.

A prediction of the intensity of friction on the surface of a 6 in. cylinder, immersed in an airstream having a speed of 30 ft. per sec. is given by Mr. Green in R. & M. 1313. To allow direct comparisons, predictions of the intensity of friction have been made by the methods described in R. & M. 1314 and in R. & M. 1176 (Dr. Thom), from the same experimental data used by Mr. Green. The three predictions are compared in Fig. 6, where values of ($f/\varrho V_0^2$) are plotted against $\theta°$. The predictions obtained by the methods of R. & M. 1313 (Green) and R. & M. 1314 (Falkner and Skan) respectively are in very close agreement over practically the entire range of θ for which the flow in the boundary layer is laminar. There is, therefore, little to choose between the two methods in so far as accuracy of prediction of surface friction is concerned. In application, however, the method of R. & M. 1314 appears to be the quicker and for this reason this method has been used to predict the theoretical distributions of surface friction given later in the paper.

* "The Boundary Layer of the front portion of a cylinder."

† R. & M. 1313. "Viscous Layer associated with a circular cylinder."

‡ "Some approximate solutions of the Boundary Layer equations."—V. M. Falkner and Miss S. Skan. R. & M. 1314.

The results obtained at the front of the cylinder by Dr. Thom's method are seen to be in very close agreement with those obtained by the other two methods, but beyond $\theta = 45°$, the known limitations of the solution influence the results, which are obviously in error.

Velocity Gradient at Surface.—It will be recalled that in earlier work on an aerofoil (R. & M. 1315) the velocity gradient at the surface was taken to be $(V/\bar{y})$, where V was the velocity measured with a surface tube at a distance $\bar{z}$ of 2 to 3 thousandths of an inch from the surface ; and it was shown that, in general, this assumption gave satisfactory results. It is obvious, however, that this assumption is only permissible provided the boundary layer is not too thin. It can be estimated from the experimental data given in R. & M. 1179* that the thickness (δ) of the boundary layer on a cylinder at $\theta = 45°$ is given by the relation $10^3\delta/D = 5 \cdot 2 - 0 \cdot 57 \times 10^{-5} (V_0 D/\nu)$ for values of $(V_0 D/\nu)$ within the range covered in the present experiments. The thickness of the boundary layer at $\theta = 45°$ on the smaller cylinder (2·93 in.) was therefore about 0·014 in., and on the larger cylinder (5·89 in.) about 0·025 in.† The assumption that the velocity gradient at the surface is given by $(V/\bar{y})$, where $\bar{y} = 0 \cdot 0025$ in. (mean value) implies therefore that there is a linear distribution of velocity across the inner 18 per cent. of the thickness of the boundary layer at $\theta = 45°$ on the 2·93 in. cylinder and across the inner 10 per cent. of the thickness on the 5·89 in. cylinder. It appears necessary then to inquire into the accuracy of this assumption. For the purpose of this enquiry several radial distributions of velocity near the surface of each cylinder at $\theta = 30°$ and 50° have been determined by the method due to Dr. Thom. These distributions of velocity are given by the curves in Fig. 7. The tangents at the surface to these velocity curves are given by the dotted lines. In all cases, the velocity curves are slightly convex upwards, and so a value of $(V/\bar{y})$ — the value of $\bar{y}$ taken is 0·0025 in.—underestimates the velocity gradient at the surface. Values of $\left(\frac{\partial V}{\partial y}\right)_{y=0}$ and of $(V/\bar{y})$ obtained from the curves of Fig. 7 are collected in Table I. It is seen in the last column of this table that the ratios of $\left(\frac{\partial V}{\partial y}\right)_{y=0}$ to $(V/\bar{y})$ are fairly constant. This constant ratio can be taken to be 1·16. The theoretical relation is therefore $\left(\frac{\partial V}{\partial y}\right)_{y=0} = 1 \cdot 16\ (V/\bar{y})$.

---

* loc cit.

† It is of interest to mention here that the thickness of the boundary layer on the aerofoil at a distance of only 0·05 of the chord from the nose was 0·04 in. at 80 ft. per sec. and 0·05 in. at 60 ft. per sec.

TABLE I.

$\bar{y} = 0 \cdot 0025$ inch.

D ins.	V_0 ft./sec.	$\theta°$	Theory (Thom). V at $\bar{y}$ ft./sec.	$\left(\frac{V}{\bar{y}}\right)$ (b)	$\left(\frac{\partial V}{\partial y}\right)_{y=0}$ (a)	Ratio. (a)/(b)
2·93	71·9	50	44·9	$2 \cdot 16 \times 10^5$	$2 \cdot 53 \times 10^5$	1·17
5·89	71·9	50	36·0	1·73	1·97	1·14
5·89	71·9	30	26·3	1·26	1·46	1·16 } 1·16
2·93	41·0	50	19·6	0·93	1·07	1·15
2·93	41·0	30	14·4	0·69	0·80	1·16

The question which now arises is whether the above theoretical relation holds in practice. No direct evidence on this matter can obviously be obtained, but it is to be expected that if the measured and theoretical velocity distributions are in agreement in the outer part of the boundary layer they will also be in agreement close to the surface. The curves given in Fig. 8 show that the velocity distribution measured in the outer part of the boundary layer on an 8·9 in. cylinder (*see* R. & M. 1179) is in close agreement with that predicted by Dr. Thom's method. It is concluded then that the relation $\left(\frac{\partial V}{\partial y}\right)_{y=0} = 1 \cdot 16\ (V/\bar{y})$ obtained from theoretical considerations can be used to predict the velocity gradients at the surface from the experimental values of $(V/\bar{y})$. The intensity of friction on the surfaces of the 2·93 in. and 5·89 in. cylinders was therefore determined by substituting the experimental values of $(V/\bar{y})$ in the relation $f = 1 \cdot 16\ \mu\ (V/\bar{y})$.

Theory and Experiment Compared.—Comparisons of the measured distributions of frictional intensity $(f/\varrho V_0^2)$ around the two cylinders with those predicted by the method of R. & M. 1314 are given in Fig. 9. The agreement between theory and experiment is seen to be reasonably close for the 5·89 in. cylinder* but less satisfactory for the 2·93 in. cylinder. Since the theoretical predictions for the two cylinders are consistent in themselves, it would seem that the accuracy of measurement of the frictional intensity on the smaller cylinder is not so good as that on the larger cylinder. It follows then that a conclusion which may be drawn from the comparisons

* It should be noted that the comparisons for the 5·89 in. cylinder cover the sensitive range of $(V_0 D/\nu)$.

is that reliable measurements of friction with the surface tubes can only be obtained provided that the boundary layer is not too thin, and that this condition is not satisfied on the 2·93 in. cylinder.

Drag.—Values of the drag coefficients of each cylinder estimated from the measurements of normal pressure and of surface friction are given in Table II. The drag coefficients due to the normal pressure were obtained from the expression

$$K_D = \int_0^{\pi} \frac{(p - p_0)}{\varrho V_0^2} \cos\theta \, d\theta$$

and those due to the surface friction from the expression

$$K_D = \int_0^{\pi} \frac{f}{\varrho V_0^2} \sin\theta \, d\theta$$

The drag coefficients for the cylinders in an infinite stream predicted from the tunnel results are given in the last column of Table II. The corrections for the interference of the tunnel walls on the drag were taken from the curves in Fig. 7 of R. & M. 1223*. The results given in Table II show that the contribution of surface friction to the

TABLE II.

$\varrho = 0{\cdot}00232$ slugs/ft.^{3} $\nu = 0{\cdot}0001665$ ft.^{2}/sec.

D ins.	V_0 Ft./sec.	$\frac{V_0 D}{\nu}$	K_D (Tunnel).			K_D Infinite stream.
			From normal pressures.	From surface friction.	Total.	
	Normal Stream of Tunnel.					
5·89	71·9	$2{\cdot}12 \times 10^5$	0·262	0·0053	0·267	0·252
5·89	56·4	1·66	0·391	0·0053	0·396	0·373
5·89	35·8	1·06	0·618	0·0050	0·623	0·587
2·93	71·9	1·06	0·609	0·0041	0·613	0·606
2·93	56·5	0·83	0·602	0·0046	0·607	0·601
2·93	41·0	0·60	0·594	0·0055	0·600	0·594
	Disturbed Stream behind Rope Netting.					
5·89	56·9	$1{\cdot}68 \times 10^5$	0·164	0·0089	0·173	0·163
5·89	36·5	1·08	0·235	0·0075	0·243	0·229
2·93	41·0	0·60	0·466	0·0068	0·473	0·468

* On the two-dimensional flow past a body of symmetrical cross-section mounted in a channel of finite breadth.—Fage.

drag of a cylinder is very small. Thus, at the lowest Reynolds number of $0 \cdot 60 \times 10^5$ (normal stream) the contribution amounts to about $0 \cdot 9$ per cent. of the total drag, and at the highest Reynolds number of $2 \cdot 12 \times 10^5$ to about $2 \cdot 0$ per cent. The values of K_D (infinite stream) given in the last column of Table II are plotted against $\log_{10}$ (VD/ν) in Fig. 10. The dotted lines in this figure have been plotted from the results of some earlier experiments made on an 8·9 in. cylinder over the same range of Reynolds number. The present results exhibit the same characteristics as those shown by the earlier results, and in particular the lateral displacement of the drag curve due to the disturbances from the rope netting is about the same.

Comparison of Pressure Curves taken in the Normal and Disturbed Streams.—It is shown in Fig. 10 that adding disturbances to the normal stream of the wind tunnel causes the sensitive range of Reynolds number to occur earlier, and without any appreciable modification to the shape of the K_D curve over this sensitive range. It is thought to be of some interest to compare the pressure distributions measured in the two streams at the appropriate values of (VD/ν) corresponding to selected values of K_D taken on the rising and falling parts of the two drag curves. To obtain the data needed for these comparisons, measurements have been made of the distribution of pressure around the median section of the 8·9 in. cylinder mounted vertically, with very small clearances at its ends, between the roof and floor of the 4 ft. tunnel. Fifteen distributions of pressure were measured, of which nine were taken with the cylinder mounted in the normal stream of the tunnel, and six with the cylinder mounted in the disturbed stream about 36 in. behind the square-meshed rope netting. The ranges of wind speed covered in the experiments were 22–72 ft. per sec. (normal stream) and 16–58 ft. per sec. (turbulent stream).

The pressure observations taken in both the normal and disturbed streams were first faired by plotting values of the pressure coefficient $(p - p_0)/\rho V_0^2$ against V_0 at a constant value of $\theta°$. The curves of pressure distribution given in Fig. 11 (b—e) were then obtained from values taken from these faired pressure curves. Values of the drag coefficient K_D were estimated from the experimental distributions of pressure. These values of K_D, for both the normal and disturbed streams, are plotted against V_0 in Fig. 11 (a).

The comparisons between the pressure distributions for the normal and disturbed streams, for several values of K_D are given in Fig. 11 (c—e). The following conclusions can be drawn from these comparisons. When the value of K_D is taken on the falling parts of the drag curves (reference letters on the curves are B, B′ (c) ; F, F′ (e) ; and D, D′ (d)) the pressure distributions are in close agreement. On the other hand, when the value of K_D is taken on the rising parts of the drag curves (F_0, F_0' (e) ; D, D_0 (d)), or on the falling part of one curve and on the rising part of the other curve (F, F_0' (e) ; F′, F_0 (e) ; D′, D_0 (d)) the pressure distributions differ. An exception arises however from the comparison for the value of K_D at the point of intersection of the drag curves (D and D_0') for the pressure distributions are then almost the same. The curves of Fig. 11 (b) have been included to show the progressive change in the pressure distribution associated with the large drop in the drag coefficient.

General Survey of Results.—A résumé of the salient features of the flow around a circular cylinder can now be given.

(*a*) *Normal Stream.*—The most important feature revealed by the measurements of normal pressure and surface friction on the 2·93 in. cylinder is that over the range of Reynolds number characterised by a constant drag coefficient, the boundary layer leaves the surface abruptly and before a transition from laminar to turbulent flow in the layer has had time to develop to any appreciable extent. Consequently the flow characteristics, with the exception of the surface friction, are not sensibly affected by a change in the value of Reynolds number. On the other hand, the experiments on the 5·89 in. and 8·9 in. cylinders show that a progressive change in the flow characteristics takes place over the sensitive range of Reynolds number. With an increase of Reynolds number over this range, the boundary layer becomes thinner, the pressure coefficient $(p - p_0)/\rho V_0^2$ falls to a greater negative value, and the point of maximum negative pressure moves further around the cylinder. At the higher values of $(V_0 D/\nu)$ a transition from laminar to turbulent flow occurs about 10° beyond the point of maximum negative pressure, and the local conditions are such that no abrupt separation of the boundary layer from the surface takes place. In fact, the turbulent boundary layer clings to the surface for an appreciable distance around the back of the cylinder, but eventually the retarding influence of the opposing pressures leads to a complete separation of the layer from the surface and the formation of the stagnant region at the back of the cylinder.

(*b*) *Disturbed Stream.*—Disturbances in the general stream cause the sensitive range of Reynolds number to occur earlier. The changes of flow such as the increased fall in the pressure coefficient, the extension of the region of laminar flow in the boundary layer, and the delay in the separation of the layer from the surface, experienced with an increase of Reynolds number over the sensitive range in the normal stream are also experienced over the earlier range in the disturbed stream ; and it would seem that the disturbances in the general stream behave as if they were assisting the boundary layer against the opposing pressures near the surface of the cylinder.

TABLE III.

Values of $(p - p_0)/\varrho V_0^2$.

Cylinders in normal stream of 4-ft. tunnel.

Results uncorrected for interference of tunnel walls.

	5·89-in. cylinder.			2·93-in. cylinder.		
V_0 ft./sec.	71·9	56·4	35·8	71·9	56·5	41·0
$\left(10^{-5} \times \frac{V_0 D}{\nu}\right)$	2·12	1·66	1·06	1·06	0·83	0·60
$\theta = 0$	0·500	0·495	0·495	0·497	0·490	0·495
5	0·486	0·484	0·480	0·484	0·481	0·483
10	0·443	0·444	0·444	0·448	0·446	0·449
15	0·369	0·378	0·379	0·389	0·386	0·391
20	0·284	0·290	0·293	0·308	0·306	0·309
25	0·173	0·180	0·187	0·209	0·207	0·214
30	0·036	0·053	0·070	0·097	0·100	0·100
35	—0·099	—0·089	—0·061	—0·028	—0·024	—0·022
40	—0·252	—0·230	—0·194	—0·155	—0·151	—0·147
45	—0·403	—0·375	—0·332	—0·285	—0·276	—0·276
50	—0·552	—0·523	—0·453	—0·407	—0·397	—0·391
55	—0·697	—0·654	—0·566	—0·511	—0·498	—0·495
60	—0·829	—0·768	—0·656	—0·597	—0·585	—0·578
65	—0·933	—0·867	—0·724	—0·658	—0·637	—0·626
70	—1·015	—0·941	—0·730	—0·691	—0·649	—0·643
72	—1·044	—	—0·724	—0·680	—0·644	—0·628
74	—1·067	—0·977	—0·712	—0·637	—0·621	—0·612
76	—	—	—0·690	—0·633	—0·601	—0·590
77	—	—0·977	—	—	—	—
78	—	—	—0·652	—0·612	—0·572	—0·572
80	—1·095	—0·959	—0·638	—0·581	—0·558	—0·560
82	—	—0·934	—0·622	—0·574	—0·548	—0·540
84	—1·082	—0·893	—	—	—	—
85	—	—0·893	—0·618	—0·567	—0·540	—0·531
86	—1·050	—0·876	—	—	—	—
88	—1·021	—0·851	—	—	—	—
90	—0·980	—0·851	—0·618	—0·567	—0·540	—0·531
92	—0·945	—	—	—	—	—
95	—0·929	—0·834	—	—	—	—
100	—0·857	—0·769	—0·629	—0·567	—0·544	—0·536
105	—0·706	—	—	—	—	—
110	—0·531	—0·619	—0·607	—0·567	—0·544	—0·536
115	—0·434	—	—	—	—	—
120	—0·387	—0·528	—0·616	—0·567	—0·551	—0·543
130	—0·340	—0·469	—0·611	—0·575	—0·560	—0·562
140	—0·324	—0·448	—0·618	—0·582	—0·575	—0·574
150	—0·312	—0·434	—0·638	—0·614	—0·590	—0·583
160	—0·304	—0·424	—0·658	—0·614	—0·608	—0·600
170	—0·304	—0·404	—0·656	—0·623	—0·617	—0·596
180	—0·299	—0·395	—0·656	—0·628	—0·612	—0·595

5".89 CYLINDER.

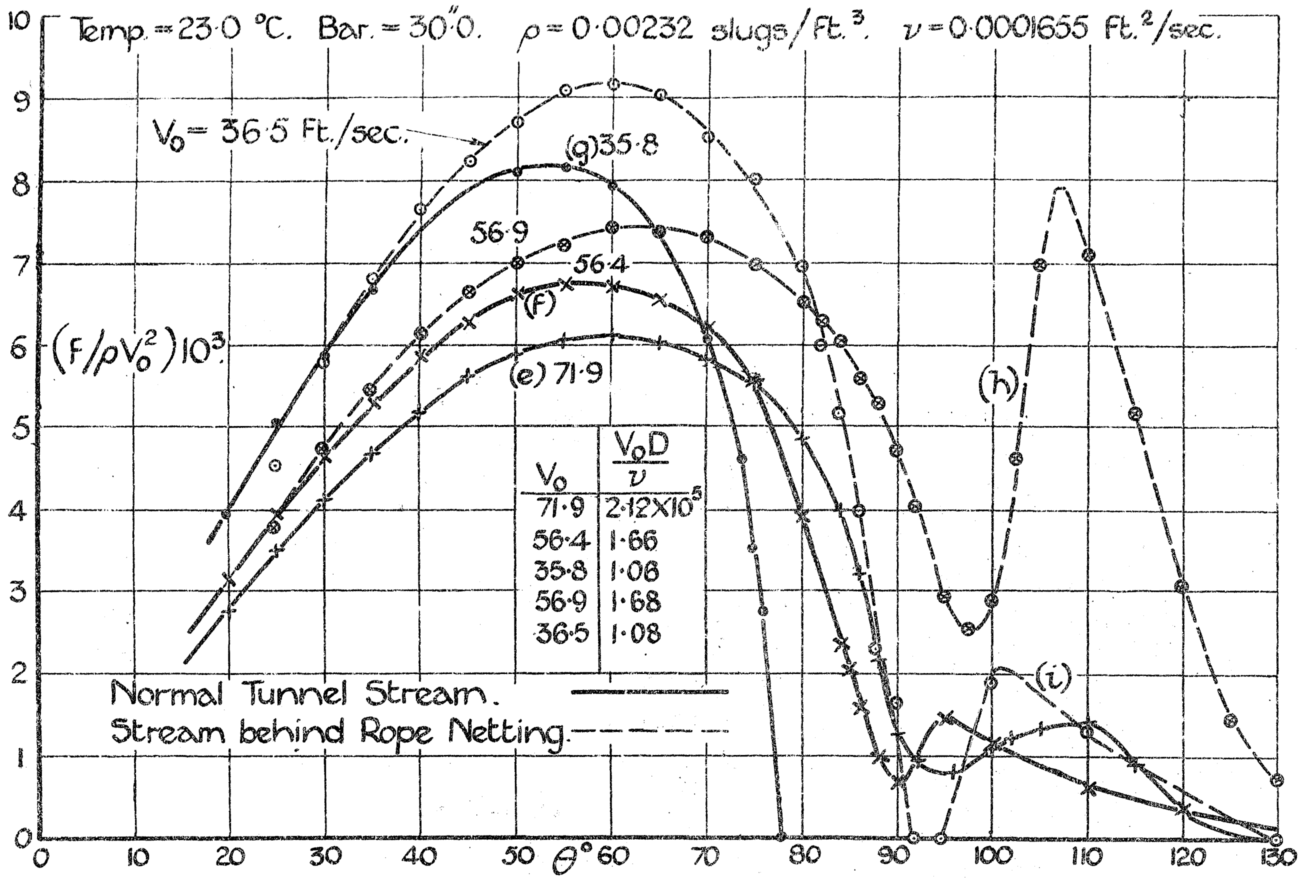

FIG. 1.

P.4159.95 A 6003.2114.775.7/31

Malby & Sons, Photo-Lith.

Temp = 23°0 C. Bar = 30"0. ρ = 0·00232 slug/ft³. ν = 0·0001655 ft²/sec.

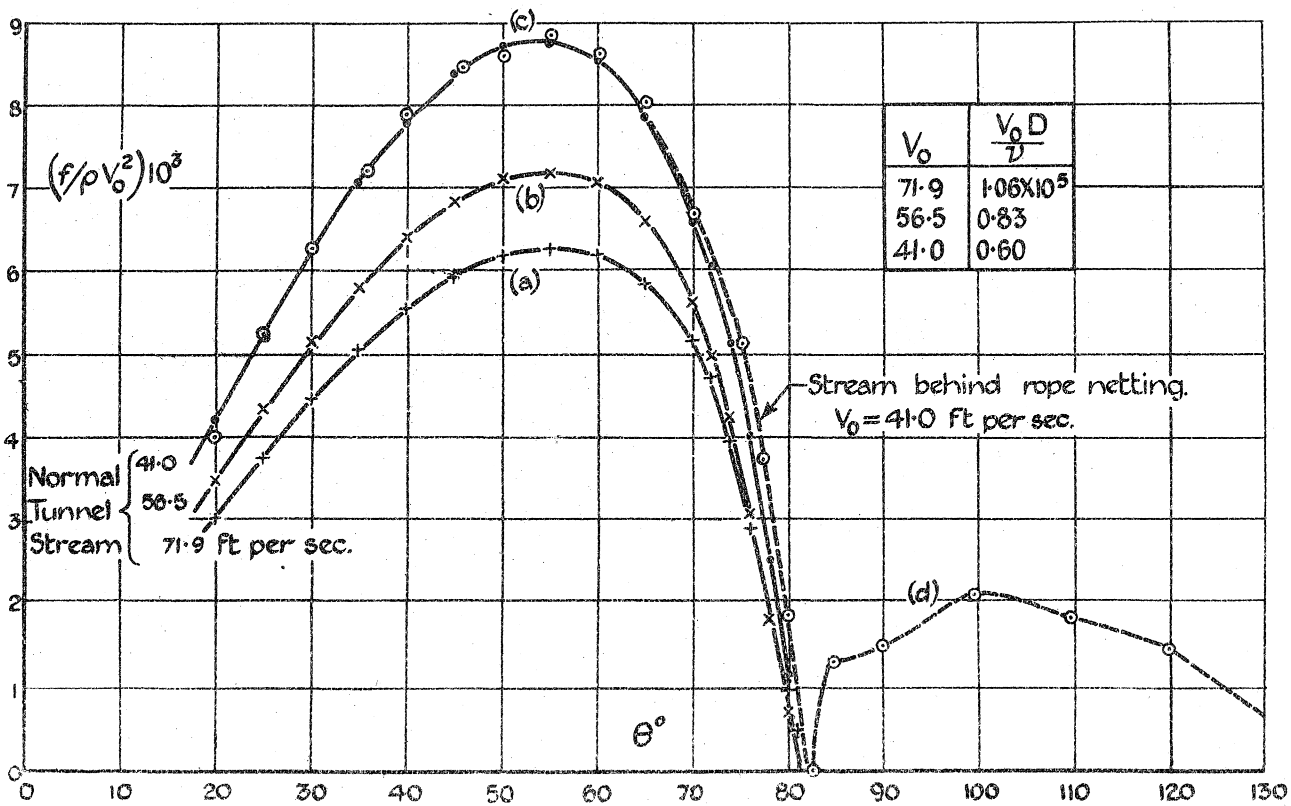

R.& M. 1369.

2.93" CYLINDER.

FIG. 2.

FIG. 3.

Results uncorrected for Tunnel-Wall Interference.

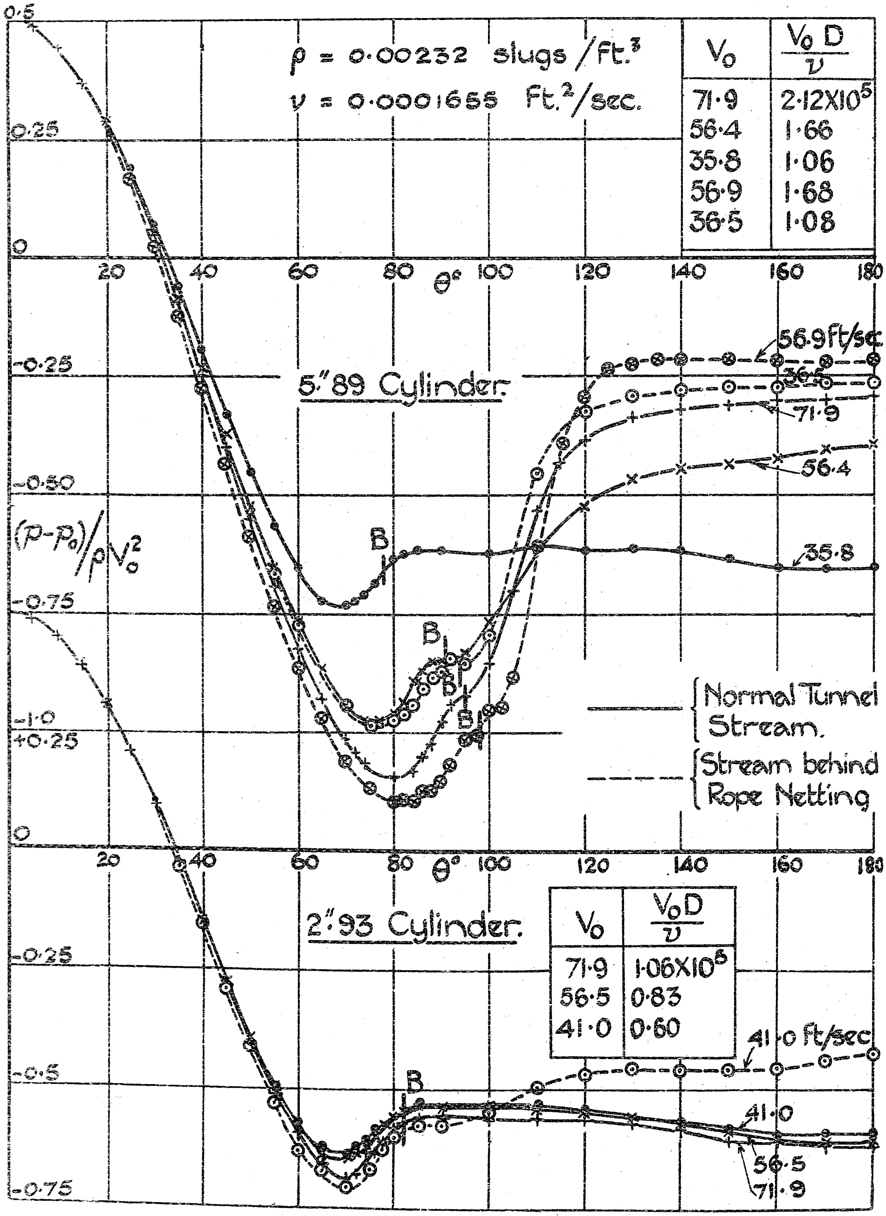

R.&M. 1369.

5·89" CYLINDER.

V_0	$\frac{V_0 D}{\nu}$
71·9	$2{\cdot}12 \times 10^5$
56·4	1·66
35·8	1·06
56·9	1·68
36·5	1·08

FIG. 4.

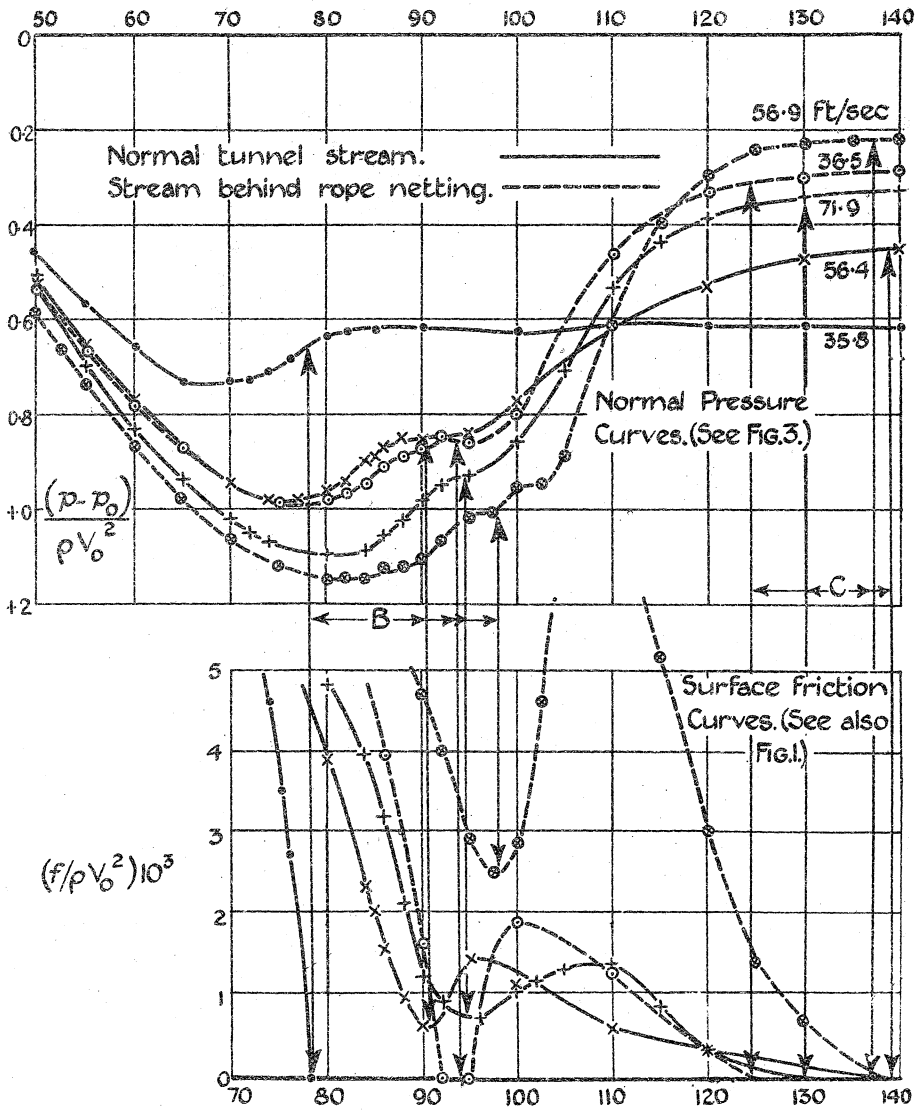

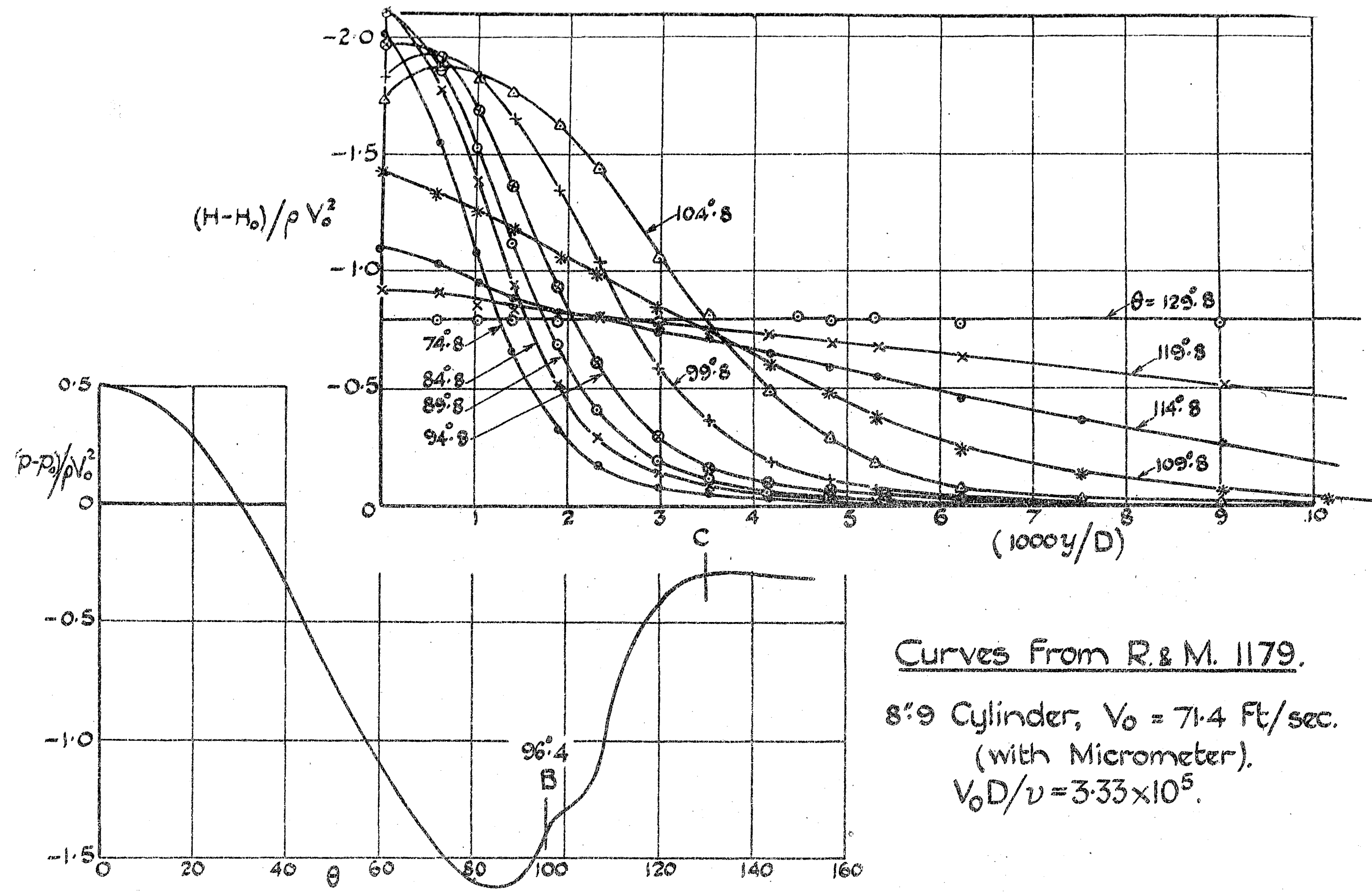

Curves From R. & M. 1179.

8"·9 Cylinder, V_0 = 71·4 Ft/sec. (with Micrometer).

$V_0 D/\nu = 3{\cdot}33 \times 10^5$.

FIG. 5.

F 4189

R.&M.1369.

THEORETICAL RESULTS FOR A 6" CYLINDER.

FIG. 6.

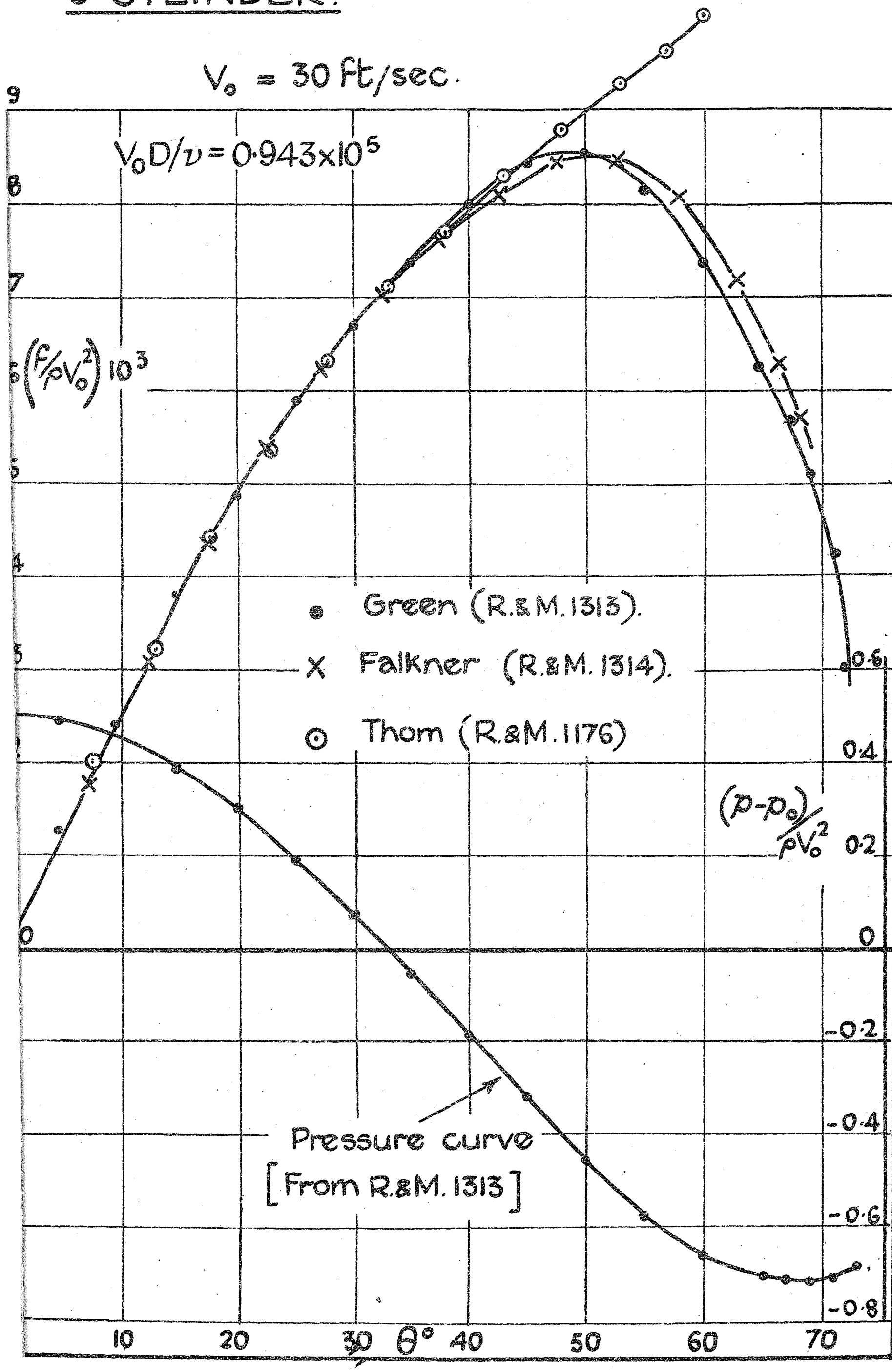

FIGS. 7&8.

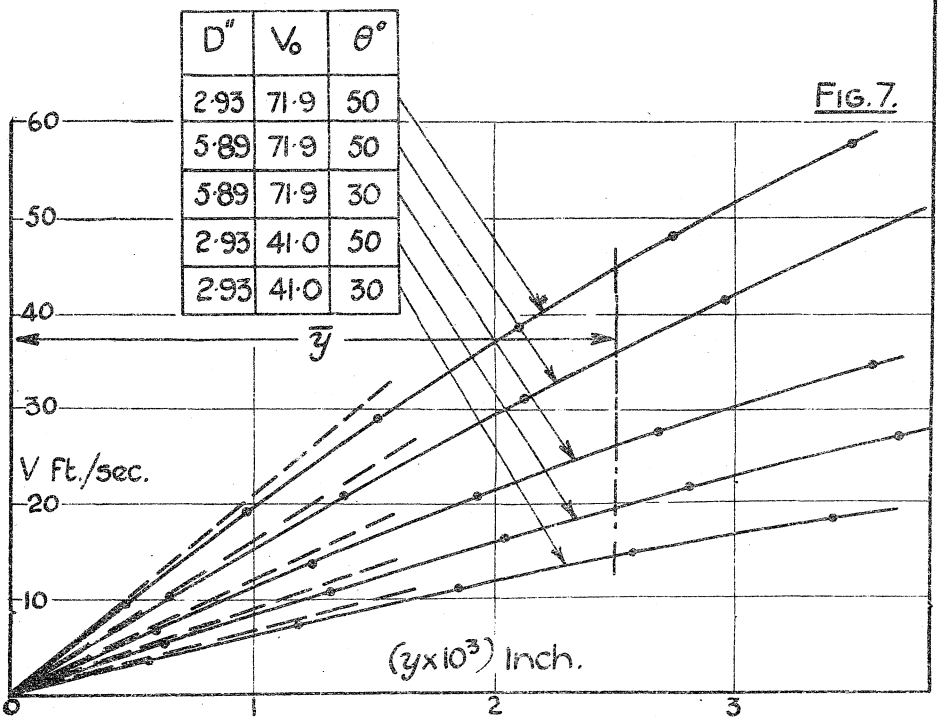

FIG. 7.

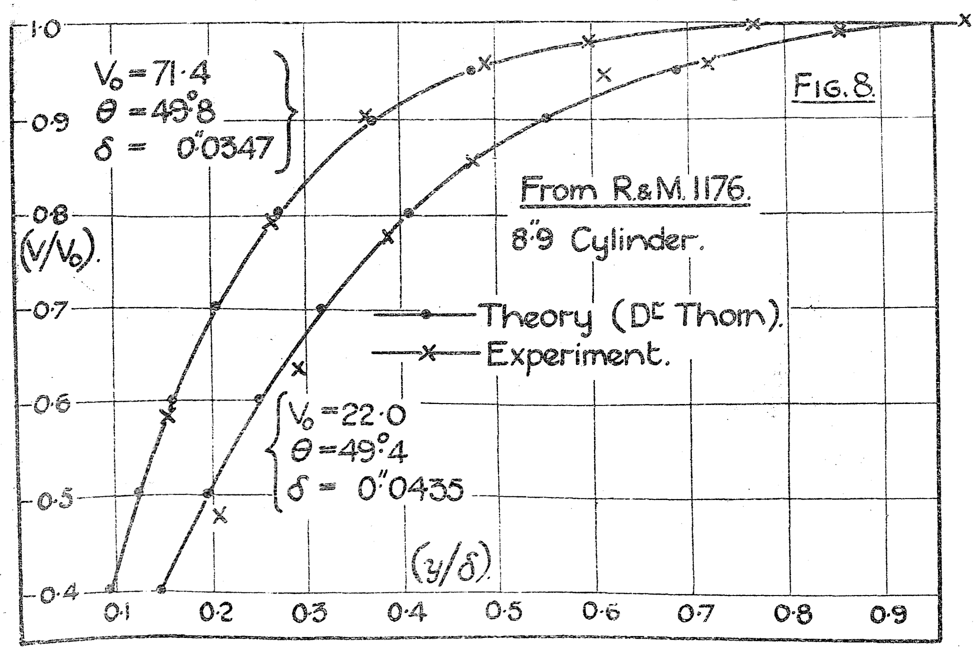

FIG. 8.

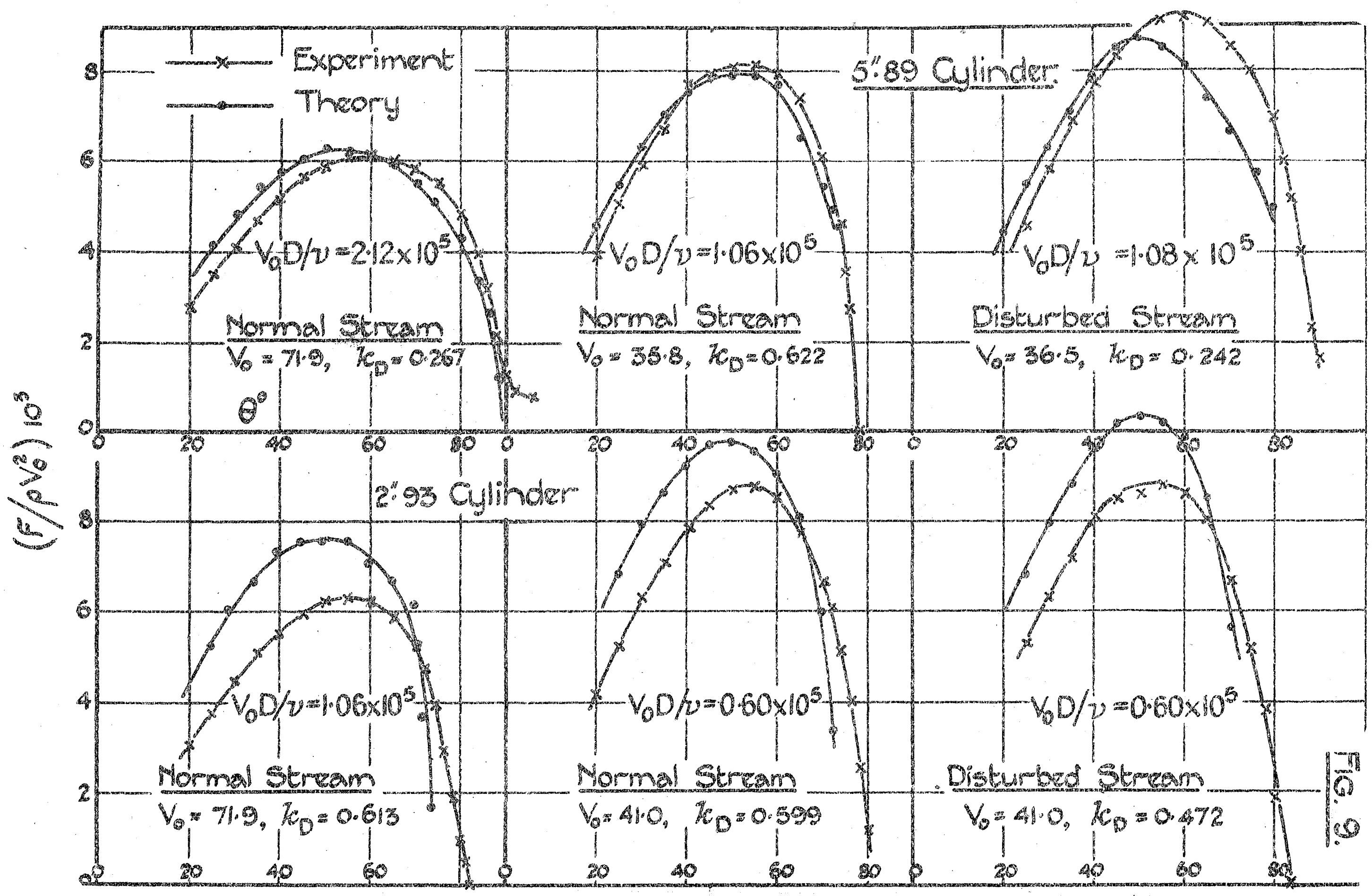

Experiment
Theory
5".89 Cylinder.
2".93 Cylinder
$(F/\rho V_0^2)\,10^3$
$\theta°$
$V_0D/\nu = 2{\cdot}12 \times 10^5$
Normal Stream
$V_0 = 71{\cdot}9,\ k_D = 0{\cdot}267$
$V_0D/\nu = 1{\cdot}06 \times 10^5$
Normal Stream
$V_0 = 35{\cdot}8,\ k_D = 0{\cdot}622$
$V_0D/\nu = 1{\cdot}08 \times 10^5$
Disturbed Stream
$V_0 = 36{\cdot}5,\ k_D = 0{\cdot}242$
$V_0D/\nu = 1{\cdot}06 \times 10^5$
Normal Stream
$V_0 = 71{\cdot}9,\ k_D = 0{\cdot}613$
$V_0D/\nu = 0{\cdot}60 \times 10^5$
Normal Stream
$V_0 = 41{\cdot}0,\ k_D = 0{\cdot}599$
$V_0D/\nu = 0{\cdot}60 \times 10^5$
Disturbed Stream
$V_0 = 41{\cdot}0,\ k_D = 0{\cdot}472$

FIG. 9.

R.& M. 1369.

Fig. 10.

CURVES OF k_D.

Infinite Stream.

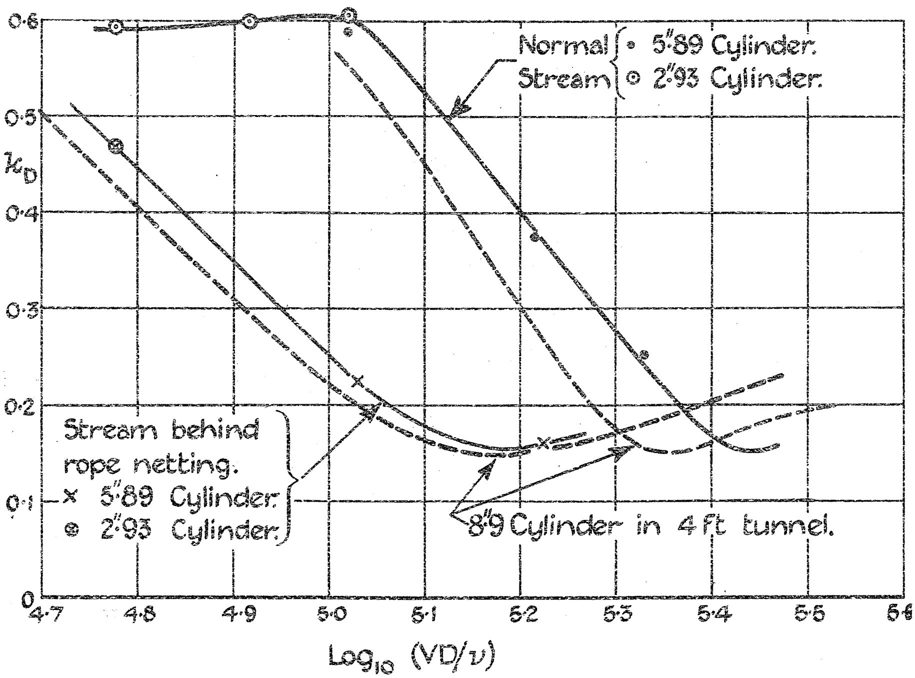

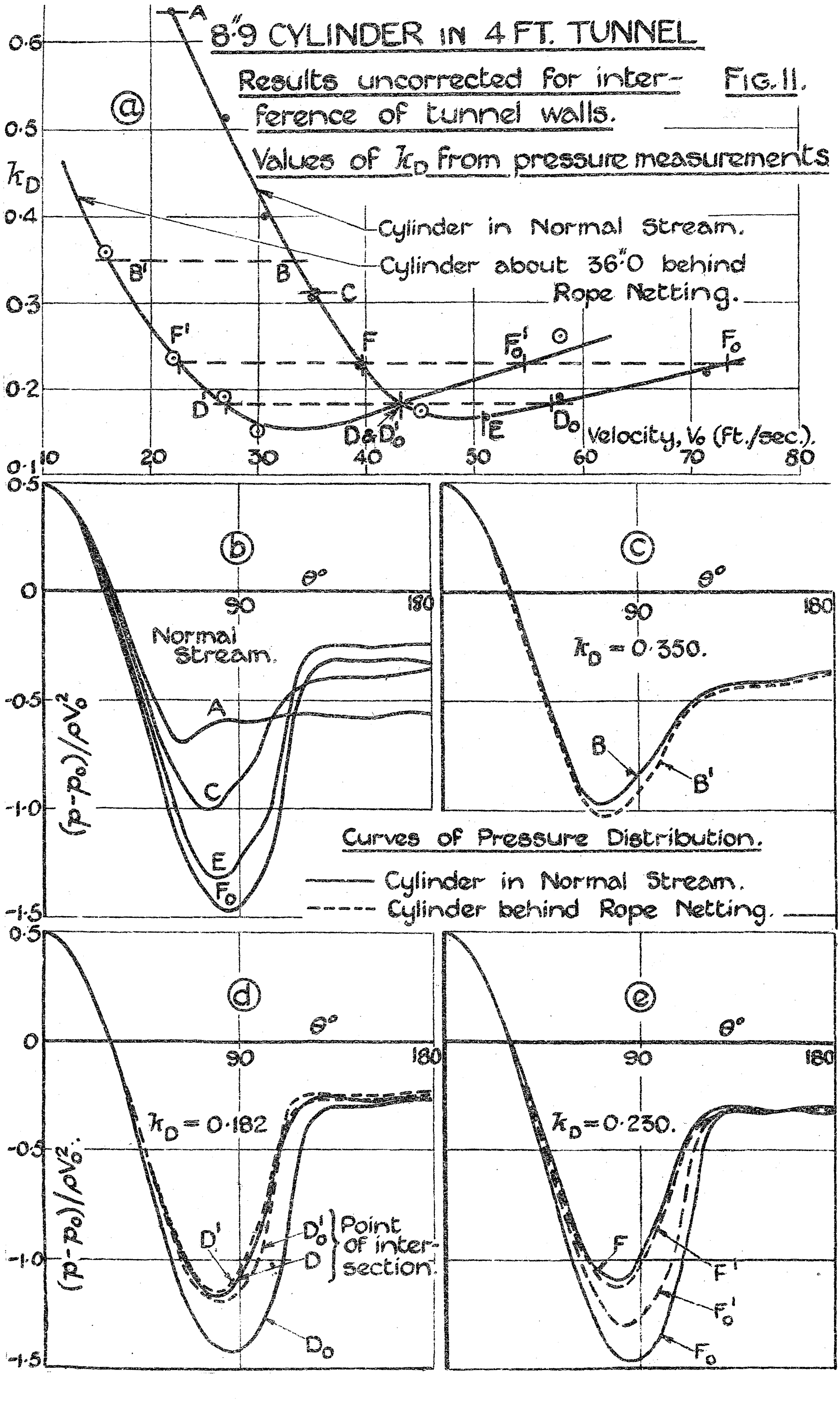

8"9 CYLINDER IN 4 FT. TUNNEL
Results uncorrected for interference of tunnel walls.
FIG. 11.
Values of k_D from pressure measurements
(a)
Cylinder in Normal Stream.
Cylinder about 36"0 behind Rope Netting.
Velocity, V_0 (ft./sec.).
k_D
(b)
Normal Stream.
(c)
k_D = 0·350.
Curves of Pressure Distribution.
Cylinder in Normal Stream.
Cylinder behind Rope Netting.
(d)
k_D = 0·182
Point of intersection.
(e)
k_D = 0·230.
$(p-p_0)/\rho V_0^2$
θ°